J Nanostruct 10(2): 362-374, Spring 2020

RESEARCH PAPER

Size Control of Ag_3PO_4 Nanoparticles Using Monoethanolamine and Oleylamine Chelating Agents

*Hind El Masaoudi [1], Ismail Benabdallah [1], Boujemâa Jaber [2], Abdelaziz Laghzizil [3], Mohammed Benaissa [1]**

[1] *Laboratory of Condensed Matter and Interdisciplinary Sciences (LaMCScI), Faculty of Sciences, Mohammed V University in Rabat, BP.1014, 10000 Rabat, Morocco*

[2] *Materials Science Facility, UATRS Division, National Center for Scientific Research (CNRST), 10000 Rabat, Morocco*

[3] *Laboratory of Applied Chemistry of Materials, Faculty of Sciences, Mohammed V University in Rabat, BP.1014, 10000 Rabat, Morocco*

ARTICLE INFO

Article History:
Received 08 October 2019
Accepted 11 February 2020
Published 01 April 2020

Keywords:
Ag_3PO_4
Monoethanolamine
Nanoparticles
Oleylamine
Size-control

ABSTRACT

In the present investigation, a systematic study on the dependence of chelating agents on the size control of silver phosphate Ag_3PO_4 powders is presented. The effect of two different capping-ligands (monoethanolamine (MEA) and oleylamine (OLA) as amino-additives) is studied using sol-gel route. Structural and morphological characterization techniques were used to quantify the particles size and molecular bonding. Results show that oleylamine as a chelating agent is more efficient in controlling the size of the as-synthesized nanoparticles, especially in low concentration of Ag^+ precursor related to its long alkyl-chain preventing nuclei assemblage. This argument is confirmed by energy interaction calculation between Ag^+ cations and oleylamine molecules using Molecular Dynamics Simulations. Finally, this investigation clearly demonstrates that the ratio between amino-additives (MEA and OLA) and Ag^+ is the key-parameter that controls the crystalline growth of Ag_3PO_4 particles thus leading to nanometric size.

How to cite this article
El Masaoudi H, Benabdallah I, Jaber B, Laghzizil A, Benaissa M. Size Control of Ag_3PO_4 Nanoparticles Using Monoethanolamine and Oleylamine Chelating Agents. J Nanostruct, 2020; 10(2):362-374. DOI: 10.22052/JNS.2020.02.015

INTRODUCTION

Nowadays, population growth and human development as well as industrial activities have led to increasing pressure on water supplies. In front of this growing shortage of water, the treatment of wastewater for reuse represents an encouraging alternative. Therefore, some studies are focused on advanced oxidation processes (AOPs) for the degradation of organic pollutants resistant to the conventional methods [1]. Among them, the photocatalytic process is a viable technology for the wastewater treatments, because it is efficient, simple and inexpensive [2]. Currently, many semiconductor-based photocatalysts have been investigated to meet the requirements of the pollution remediation. However, the photocatalytic activity of these semiconductors such as ZnO [3-4] and TiO_2 [5-6] is limited to the use of UV light of wavelengths under 400 nm, which corresponds to only 4% of the solar spectrum, and 46% of the visible sunlight between 400 and 800 nm is then not exploited. Therefore, the search for photocatalysts directly acting under visible-light irradiation is needed. Recently, Yi et al. [7-8] have reported that silver orthophosphate, Ag_3PO_4, has shown an excellent photo-oxidative

* *Corresponding Author Email: benaissa@fsr.ac.ma*

ability for O_2 generation from water splitting under visible-light irradiation, with a quantum efficiency of about 90%. However, its crystallite size remained relatively large (0.5–2 μm) thus limiting the photocatalytic performance, which is still correlated with the specific surface area of the photocatalyst [9]. The use of nanoscale particles is a way to improve the surface better. In this context, several studies have been carried out to prepare Ag_3PO_4 using different chemical methods; such as deposition–precipitation [10], an oleate-assisted method [11], co-precipitation method [12] and simple solid phase ion exchange method [13]. However, the sol–gel method remains very common for nanoparticles fabrication due to its simplicity, reliability, cheapness and high quality products. By controlling the sol–gel process and delaying crystal growth, a good control of the size and morphology of the particles can be attained. This strategy can be achieved using a surfactant implantation (chelating agent) onto the surface of the particles preventing the occurrence of agglomeration phenomena [14]. In the present paper, a systematic study on the dependence of the nature and amount of this chelating agent (capping-ligand) on the size control is presented. Two chelating agents, monoethanolamine and oleylamine, were selected by their complexing behavior and the length of carbon chains. We demonstrate that the sol-gel process based on these chelating agents is compatible to product Ag_3PO_4 nanoparticles. Due to the high content of grafted chelating agents, these materials can be chemically treated to obtain a porous photocatalyst which then opens up highly photocatalytic activities.

MATERIALS AND METHODS

Materials

All chemicals were used as received (form Aldrich Co.); silver nitrate ($AgNO_3$), sodium hydrogen phosphate (Na_2HPO_4, $2H_2O$), oleylamine (70%, OLA), monoethanolamine (99%, MEA), phosphoric acid (85%, H_3PO_4), ammonia (33%, NH3), absolute ethanol and toluene solvents (analytical grade).

Synthesis of Ag_3PO_4 powders using MEA as a complexing agent

Silver phosphate Ag_3PO_4 powders were synthesized by the sol-gel method using a mixture of $AgNO_3$ and Na_2HPO_4,$2H_2O$ solutions. A first solution was prepared by dissolving a giving concentration of $AgNO_3$ in 25 ml distilled water, followed by a controlled addition of the MEA agent aiming to complex the Ag^+ ion inhibiting therefore the growth of Ag-based nucleons. Then, a second solution was achieved by dissolving Na_2HPO_4 with an appropriate concentration in 25 mL of deionized water. This second solution was afterwards added in drops into the first one under continuous stirring for 1 h at room temperature. This solution-mixture immediately gave rise to yellow precipitates that were collected by centrifugation and successively washed with distilled water and ethanol to remove the unreacted reagents and/or by-products. Finally, the as-synthesized yellowish powders were dried at 60°C overnight in the dark.

Synthesis of Ag_3PO_4 powders using OLA

As described above and to study the effect of OLA on the crystal growth of Ag_3PO_4, two solutions were also separately prepared and then mixed in the presence of OLA molecules. The first solution of $AgNO_3$ with OLA was prepared and dissolved in 15 ml of toluene then stirred for about 1h at room temperature. A second solution of H_3PO_4 dissolved in 5 ml of ethanol was added to the first solution under vigorous stirring at room temperature. After 30 min, the resulting solution-mixture immediately gave rise to yellow precipitates which were ultrasonically re-dispersed in toluene and re-precipitated in ethanol and then centrifuged. The dark-yellow precipitate was then oven-dried. To remove OLA surfactant from Ag_3PO_4 matrix, the Ag_3PO_4 powders were gradually dispersed in a mixture of solvents, ammonia/water/ ethanol/ toluene, with stirring at room temperature. After stirring for 1 hour, the mixture was centrifuged and the precipitates were then re-dispersed in 100 ml of ethanol. To this mixture, a solution of 50 ml of ethanol containing 1 mmol of ammonia has added and then left under stirring for another hour. Finally, the centrifuged powder is only dispersed in water and the resulting powder was dried at 60°C overnight.

Techniques

The crystalline phase of Ag_3PO_4 was identified using an X-ray diffractometer (XRD) (Panalytical Expert Pro) in Bragg-Brentano geometry with Cu-Kα radiation source, while morphology and size of the particles were determined by a transmission electron microscopy (TEM, Thermo-Fisher, Talos)

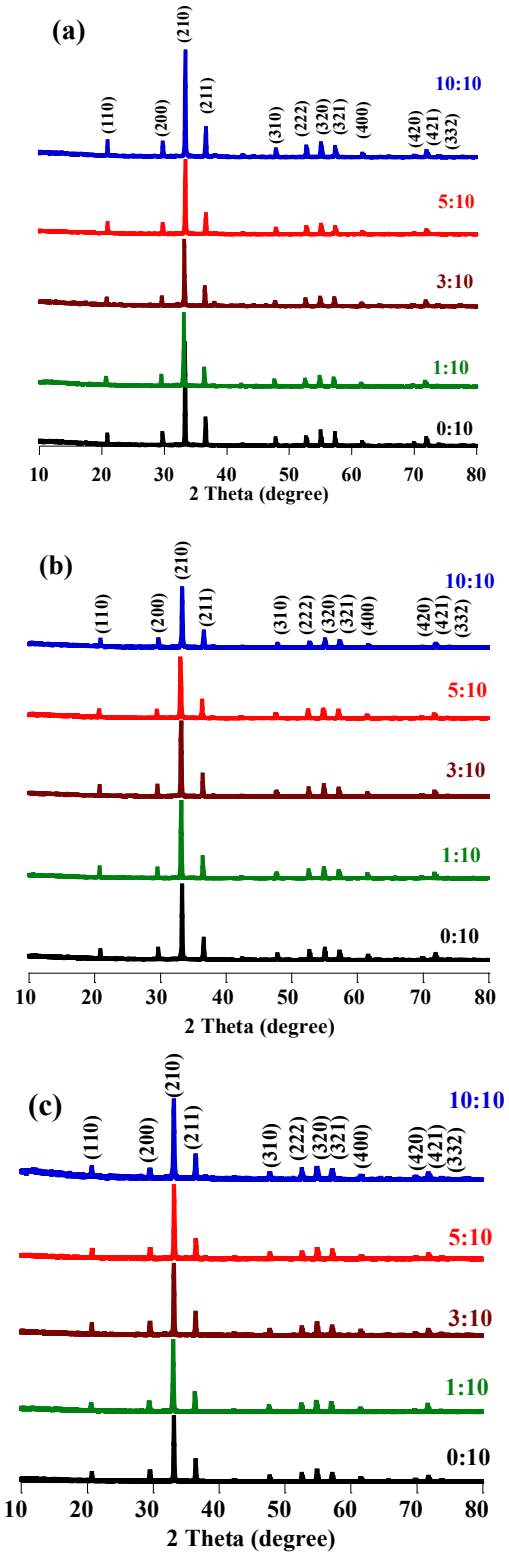

Fig. 1. X-ray diffractograms of the Ag_3PO_4 powders for Ag+ concentrations of (a) 0.005 M, (b) 0.007 M and (c) 0.01 M with different MEA:Ag^+ ratios

Table 1. Crystallite size and lattice parameter "a" of the as-synthesized Ag_3PO_4 powders using MEA as chelating agent.

[Ag^+]	MEA:Ag^+ ratio									
	0:10		1:10		3:10		5:10		10:10	
	Size (nm)	*a*(Å)	Size (nm)	*a*(Å)	Size (nm)	*a*(Å)	Size (nm)	*a*(Å)	Size (nm)	*a*(Å)
0.005M	55.6	6.0107	50.7	6.0357	46.56	6.0263	42.04	6.0234	43.48	6.0064
0.007M	51.41	6.0066	50.89	6.0220	46.62	6.0224	44.26	6.0340	44.96	6.0030
0.01M	51.59	6.0227	54.93	6.0367	45.17	6.0237	48.10	6.0187	41.11	6.0233
0.05M	45.63	6.0251	45.96	6.0268	53.76	6.0027	45.54	6.0208	43.86	6.0343
0.1M	53.81	6.0305	48.38	6.0238	54.71	6.0199	44.67	6.0035	46.86	6.0257

at an operational voltage of 200 kV, equipped with an energy dispersive spectrometer (EDS). FT-IR measurements have served to characterize and identify the functional groups of the powders as performed using a VERTEX 70 spectrometer.

RESULTS AND DISCUSSION

In the present study, the particles size of the as-synthesized Ag_3PO_4 powders was scrupulously investigated according to the precursor's concentration and the nature of chelating agent (MEA and OLA).

Effect of Mono-ethanolamine (MEA)

To better control the overall reaction conditions effect on the particles size, a series of Ag^+ concentrations (0.005M, 0.007M, 0.01M, 0.05M and 0.1M) were used. For each Ag^+ concentration, five different amounts of MEA were tested following these MEA: Ag^+ molar ratios: 0:10, 1:10, 3:10, 5:10 and 10:10.

A series of XRD patterns were performed as presented in Fig. 1. As can clearly be shown, indexation of all diffraction peaks shows the presence of the body-centered cubic structure of Ag_3PO_4 (JCPDS no. 01-071-1836). In addition, the intense and sharp peaks of all patterns indicate a good crystallinity of Ag_3PO_4 powders. No diffraction peaks resulting from impurities or secondary phases were detected, the lattice parameter "a" of the as-synthesized Ag_3PO_4 powders was determined according to:

$$a = d\sqrt{(h^2 + k^2 + l^2)} \quad (1)$$

where d=λ⁄2sinɵ is the (khl) interplanar spacing and λ is the wavelength of the used x-ray radiation (λ = 1.54056 Å for Cu-Kα radiation).The average crystallite size was estimated using the Debye Scherrer's formula [17]:

$$D = \frac{K\lambda}{\beta \cos\theta} \quad (2)$$

where K is a constant equal to 0.94, β is the peak full-width at half-maximum, and θ is the Bragg peak position. Results are reported in Table 1, indicating that the crystallite size of the Ag_3PO_4 decreases with increasing the MEA amount up to 5:10 ratio and then the size of the crystallites begins to increase beyond this ratio.

In order to examine the local molecular binding of Ag_3PO_4 particles and to verify the existence of MEA residues related by-products, FTIR spectra of selected samples are shown in Fig. 2. The absorption band at 940 cm^{-1} is due to stretching vibration of P-O bonding, while the band at 540 cm^{-1} comes from the bending vibration of O-P-O [18-19]. A broad peak of low intensity between 3000 and 3500 cm^{-1} corresponds to the vibration of OH of the adsorbed water [20]. It can clearly be seen that there are no absorption band related to the MEA molecules (Stretching vibration N-H at 3300 cm^{-1}, deformation vibration -CH_2 at 670 cm^{-1} and stretching vibration C-N at 1100 cm^{-1}). This result is also confirmed using TEM images (Fig. 3a) showing clean surfaces indicating a complete removal of MEA from powders. Similarly, nanoscale particle size has been detected, but their agglomeration prevents their clear visualization. For all samples, the chemical analyses by the energy dispersive X-ray (EDS) only confirms the presence of Ag, P and O elements (Fig. 3b). These analyzes are in good correlation with the XRD results within single Ag_3PO_4 phase.

Effect of oleylamine (OLA)

As in the case of MEA chelation, a series of Ag^+ concentrations (0.005M, 0.007M, and 0.01M) were used. For each Ag^+ concentration, five OLA amounts were tested according to the OLA:Ag^+ molar ratio (0:1, 1/2:1, 1:1, 2:1 and 3:1), recalling

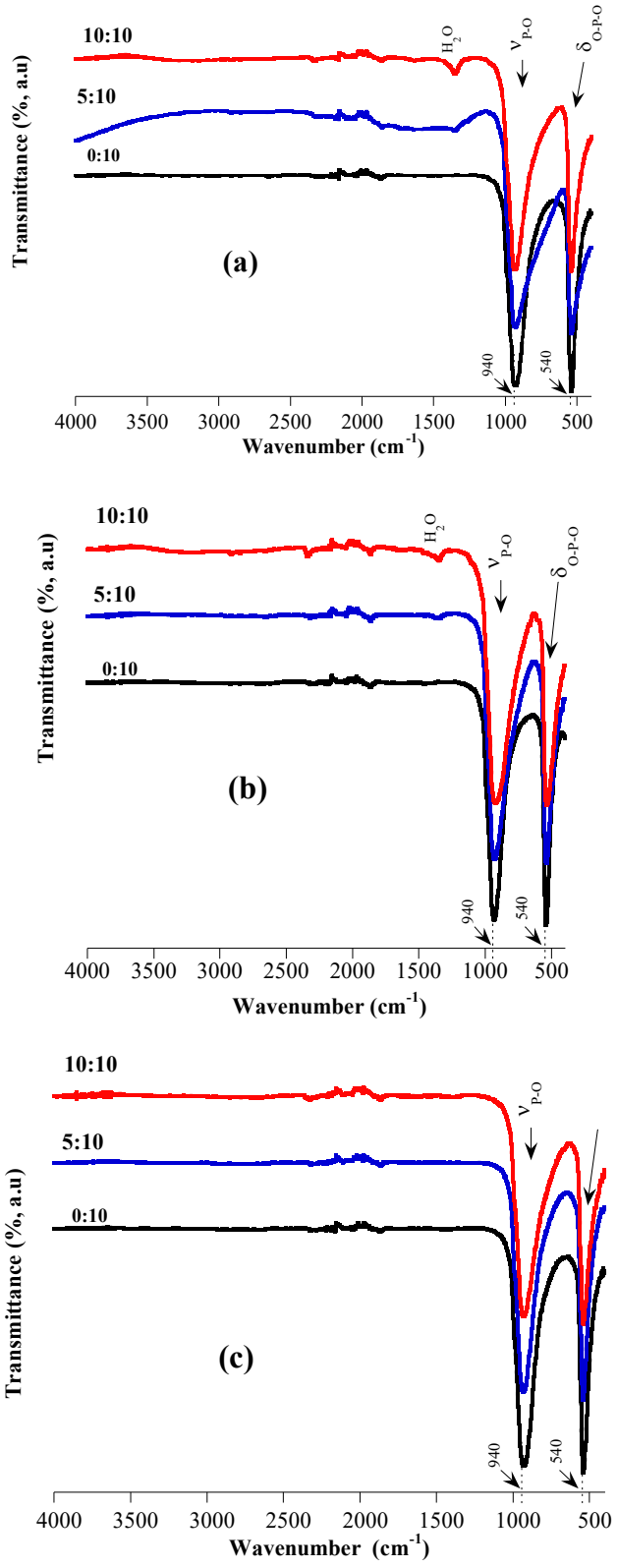

Fig. 2. FT-IR spectra of Ag3PO4 powders for Ag^+ concentrations of (a) 0.005 M, (b) 0.007 M and (c) 0.01 M with different MEA Ag^+ ratios.

that OLA has been removed from Ag_3PO_4 powders using a dilute ammonia solution.

The OLA surfactant effect was first investigated using XRD (Fig. 4) showing that all diffraction peaks were indexed in accordance with the cubic Ag_3PO_4 (JCPDS no. 01-071-1836). According to OLA content, the crystallite sizes are given in Table 2, showing that the size of the Ag_3PO_4 crystallites decreases ~~as~~ when the OLA amount increases to 2:1 ratio. Beyond this ratio, the size of the crystallites begins to increase. Fig. 5 shows IR spectra of the as-synthesized Ag_3PO_4 samples prepared at different concentrations of Ag^+ and OLA:Ag^+ molar ratios. As previously described two strong absorption bands were observed at 540 cm^{-1} assigned to the O-P-O bending vibration and at 940 cm^{-1} related to the asymmetric P-O stretching [18-19]. Peaks observed at 2920 and 2847 cm^{-1} are due to C-H asymmetric and symmetric stretching modes of the methylene group ($-CH_2$), respectively [21-22]. The appearance of these two bands indicates that a very small residual amount of C–H groups from OLA is probably present in resulting powders. This was confirmed by TEM observations (Fig. 6a-b), clearly showed the presence of an amorphous-like surface layer (organic matter) around the nanoparticles. It should be noted that this layer was irremovable even after several washing steps. As previously described, chemical analyzes by EDS lead to the detection of elements Ag, P and O constituting the Ag_3PO_4 phase whatever the synthesis method used in good agreement with the Ag_3PO_4 formulation (molar ratio Ag/P close to 3).

Comparaison between MEA and OLA effects

Before comparing the effect of MEA and OLA, we first checked the effect of the solvents used (water and toluene), without chelating agent, during the synthesis and depending on the Ag^+ concentration taken initially. As can clearly be observed from Fig. 7a, the crystallite size of the Ag_3PO_4 powders in both cases remained unchanged. This result is of great importance which justifies our strategies of the use of MEA and OLA as chelating agents for the nanoparticles size control. However, the variation trend of the crystallite size is very significant up to an MEA:Ag^+ ratio of 5:10, above which the size slightly starts to increase (Fig. 7b). Although this trend is obtained for all Ag^+ concentrations and it is important to note that the best slope is obtained for low concentrations due to their effects on the condensation kinetics during the chemical reaction [23], where Ag_3PO_4 nuclei are small enough favoring therefore a better size control. The Fig. 7c exhibits the trend of the crystallites size as a function of OLA:Ag^+ ratio. It seems that the particles size of the Ag_3PO_4 powders decreases with increasing the OLA:Ag^+ molar ratio up to 2:1 ratio, above which the size slightly increases. Although this trend is obtained for all Ag^+ concentrations, it is important to note that the best slope is again obtained for low concentrations due to the small Ag_3PO_4 nuclei. Therefore, the size of Ag_3PO_4 particles can efficiently be controlled using these two chelating agents at low Ag^+ concentration. However, the use of OLA provides even smaller nanoparticles. The observed difference between the two surfactants (MEA and OLA) in terms of their ability to control particle size is related their alkyl chain lengths. Both surfactants were used to block the crystalline growth and obtain nanoparticles. First, one can notice that the particles size control is best achieved using low Ag^+ concentrations and

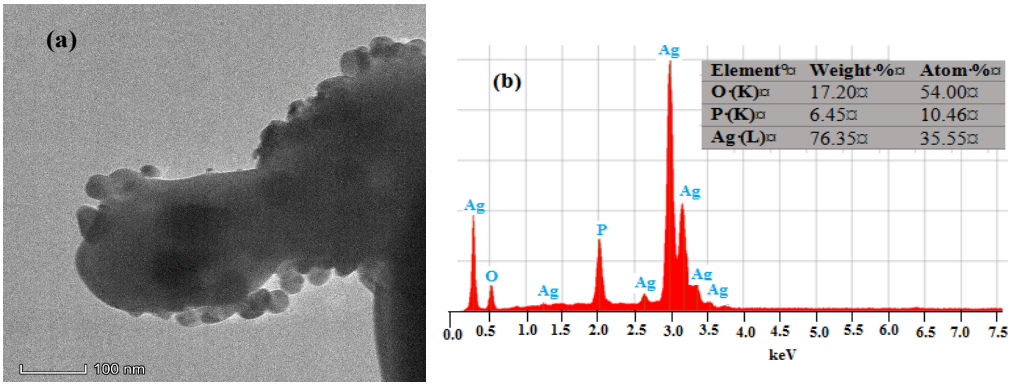

Fig. 3. (a) TEM images of Ag_3PO_4 particles synthesized with Ag^+ concentration (0.01mM) with Ag^+:MEA ratio (10:10) and (b) EDS analysis.

Table 2. Crystalline size and lattice parameter "a" as-synthesized Ag_3PO_4 powders using OLA as chelating agent.

[Ag^+]	OLA:Ag+ ratio									
	0:1		0.5:1		1:1		2:1		3:1	
	Size (nm)	a(Å)	Size (nm)	a(Å)	Size (nm)	a(Å)	Size (nm)	a(Å)	Size (nm)	a(Å)
0.005M	51.12	6.0375	52.92	6.0122	26.96	6.0301	20.58	6.0295	31.14	6.0252
0.007M	53.12	6.0213	43.68	6.0088	40.96	6.0242	29.02	6.0341	36.98	6.0145
0.01M	54.94	6.0029	46.22	6.0235	37.15	6.0390	29.49	6.0180	40.79	6.0093

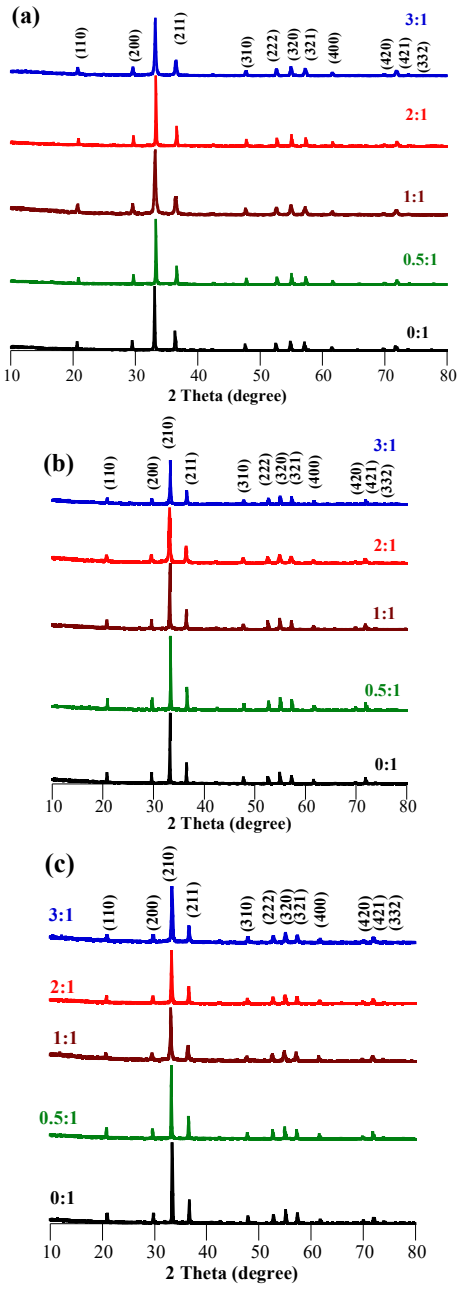

Fig. 4. X-ray diffractograms of the Ag_3PO_4 powders for Ag^+ concentrations of (a) 0.005 M, (b) 0.007 M and (c) 0.01 M with different OLA:Ag^+ ratios.

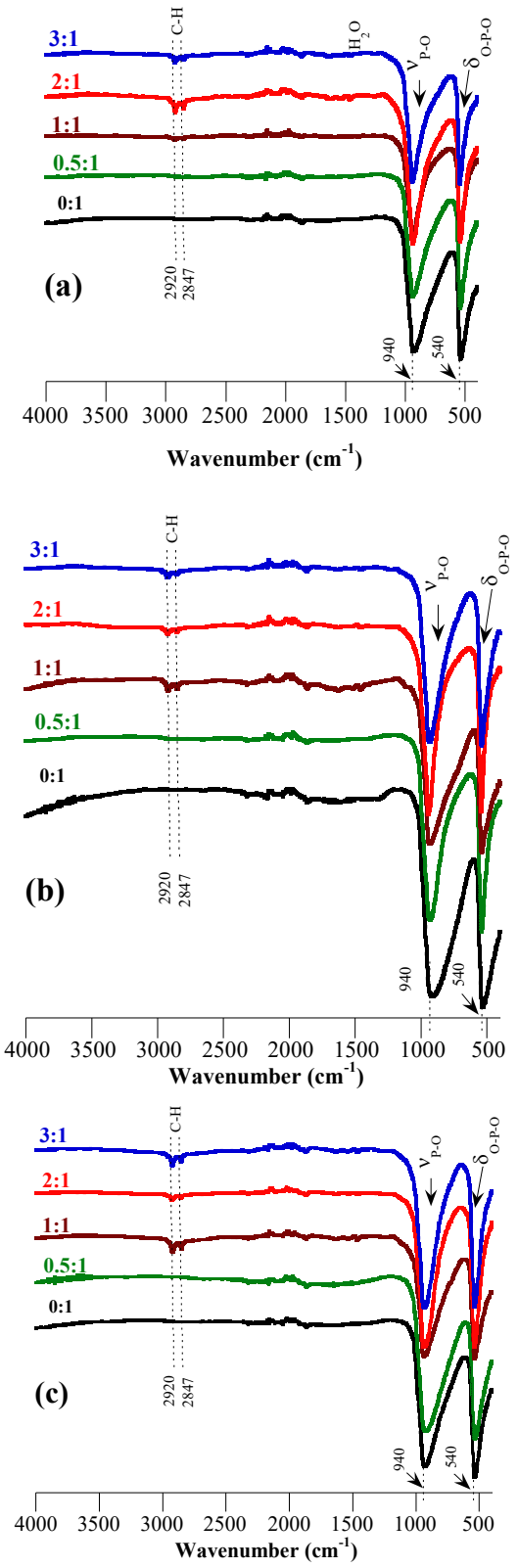

Fig. 5. FT-IR spectra of Ag_3PO_4 powders for Ag^+ concentrations of (a) 0.005 M, (b) 0.007 M and (c) 0.01 M with different OLA:Ag^+ ratios

a relatively high surfactant fraction as compared to Ag^+. However, OLA effect seems to be more efficient since our results show that particles around 20 nm in size are successfully obtained. This result can be explained on the basis of alkyl-amines interaction with the Ag_3PO_4 nanoparticles. Silver–amine complexes obtained with different alkyl-amines (MEA and OLA) are formed via the following chemical reaction process:

$$Ag^+ + 2\ R\text{-}NH_2 \longrightarrow [Ag(R\text{-}NH_2)]_2^+ \qquad (3)$$

The lone pair of electrons on nitrogen of amines coordinates with Ag^+ cations and then forms the complex. As shown in previous studies, amines having a short alkyl chain as ligands (such as MEA) have a stronger activating effect, which could bring more neighbouring nuclei at low temperature due to its weak capping effect. Therefore, amines with a long alkyl chain as ligands (such as OLA) are expected to prevent a nuclei assemblage and consequently limit the silver nanoparticles growth and yield to a narrow particles size distribution. Our arguments are indeed confirmed by calculating the energy interaction between the Ag^+ cations and MEA/OLA using Molecular Dynamics simulations. These simulations were performed with Lammps [26] by using the Verlet integration method based on Newton's motions equation with a time step of 1 fs. The temperature and pressure were controlled using the isothermal-isobaric Nose-Hoover style non Hamiltonian equations of motions. The coupling constants used for temperature control were chosen as 100 fs during the heating and relaxation runs and 500 fs during data sampling at constant temperature. A cubic simulation cell of 60*60*60 nm^3 in volume is used using periodic boundary conditions to mimic an infinite solution. Intermolecular potentials were

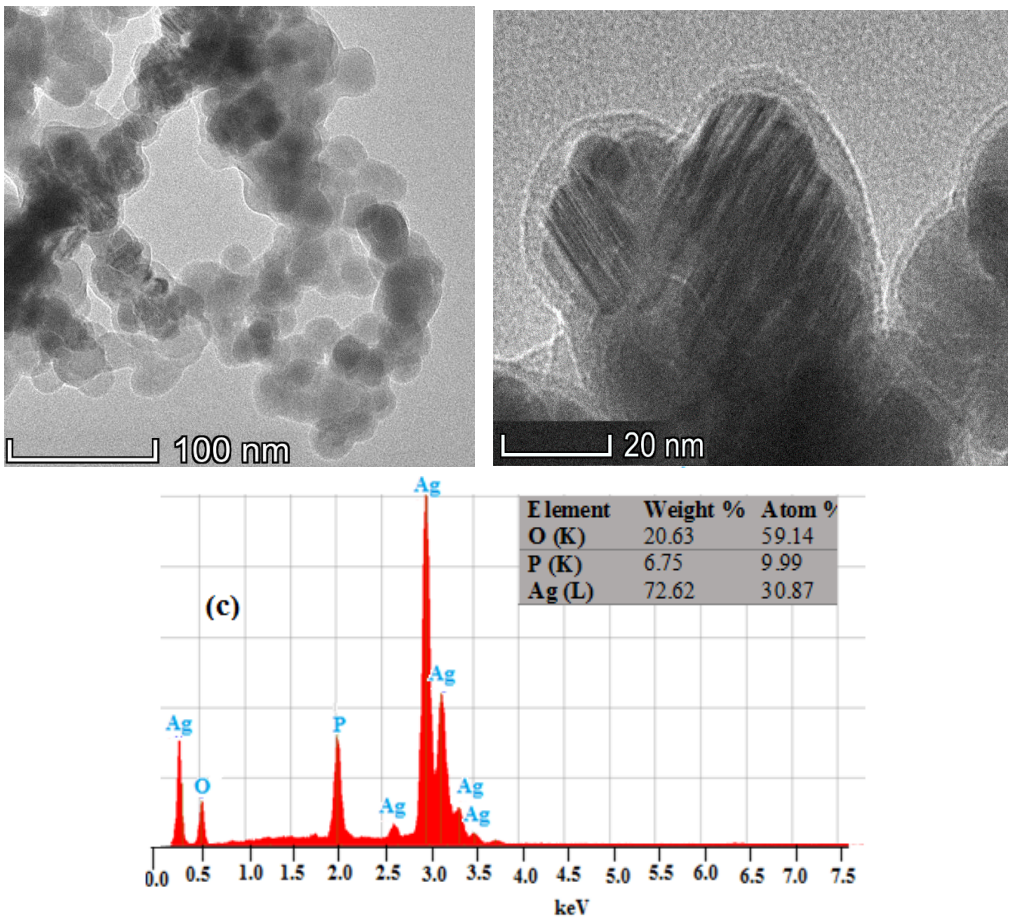

Fig. 6. TEM images of Ag_3PO_4 particles synthesized with Ag^+ concentration of 5 mM and OLA:Ag^+ ratio (2:1), (a) scale 100 nm, (b) 20 nm and (c) EDS analysis.

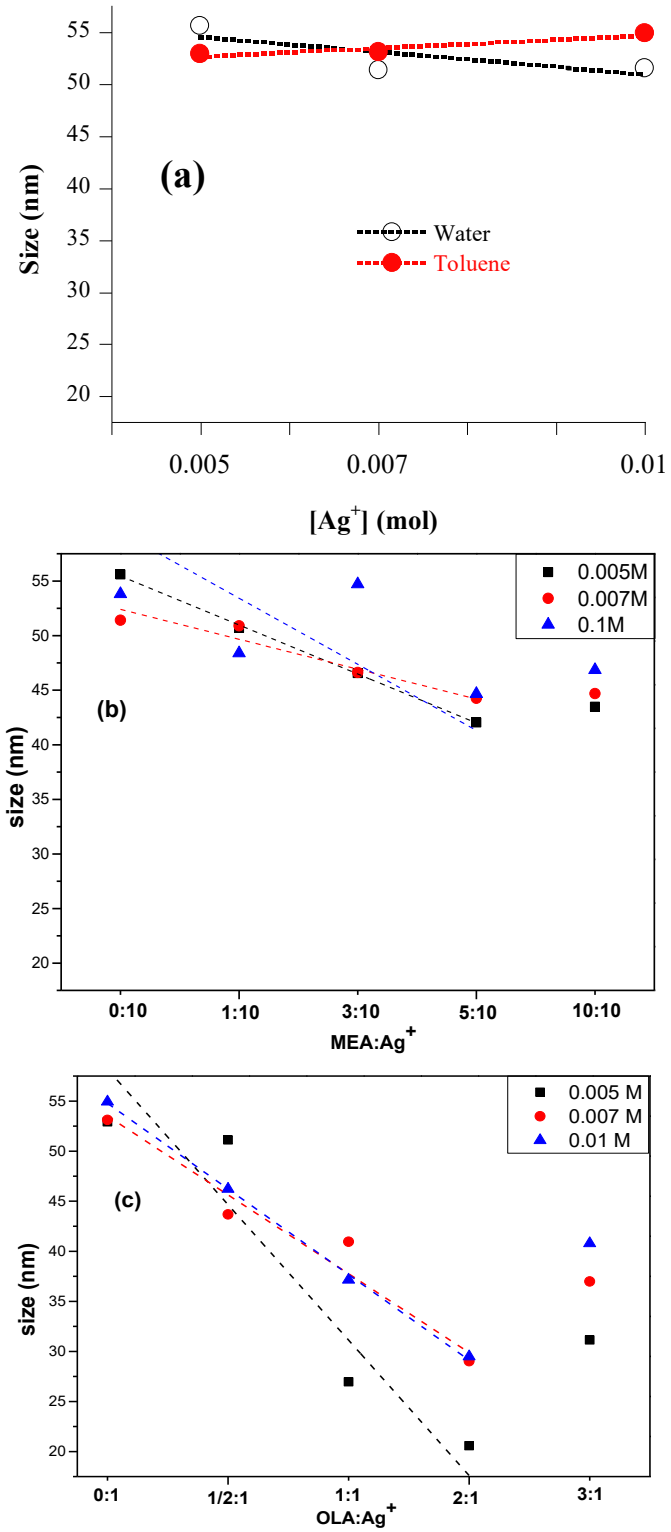

Fig. 7. Crystalline size as function (a) Ag^+ concentration of water and toluene as solvents, (b) MEA:Ag^+ ratios and (c) OLA:Ag^+ ratios of each Ag^+ concentration. The dashed lines are a guide for the eye only.

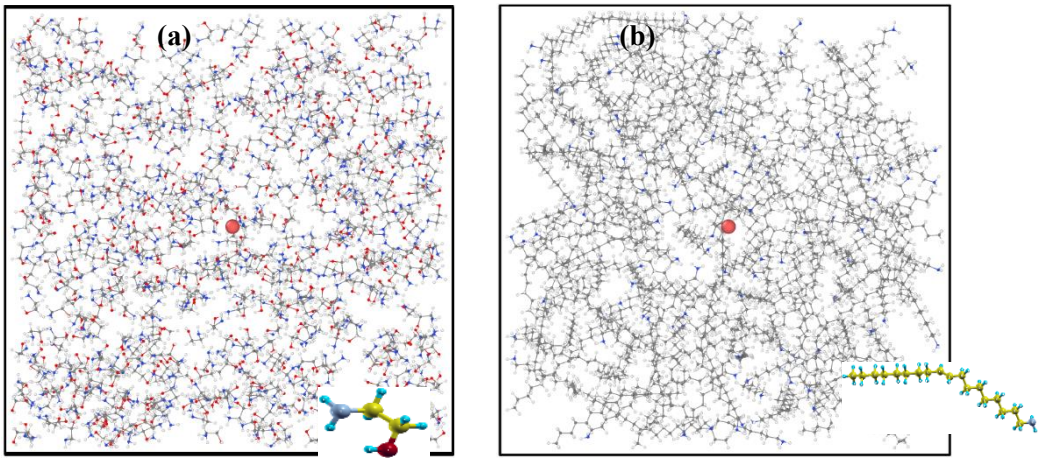

Fig. 8. Illustration of the aqueous solution mixture comprising (a) MEA, (b) OLA and a single Ag^+ ion.

Table 3. Colombian (Ec). Van Der Waals (Evdw) and the total energies between MEA. OLA and a single Ag^+ ion.

	MEA	OLA
E_T (Kcal/mol)	-86.332	-36.222
E_{Vdw} (Kcal/mol)	-17.812	-18.023
E_{coul} (Kcal/mol)	-68.515	-18.199

Table 4. Size of the as-synthesized Ag_3PO_4 powders using OLA and MEA as chelating agent compared with different Ag_3PO_4.

Preparation method	Raw materials	Additives/Complexant	Size (nm)	Reference
Precipitation	$AgNO_3$, Na_2HPO_4	-----	500	[27]
	$AgNO_3$, Na_2HPO_4	PVP	120	[28]
	$AgNO_3$, Na_2HPO_4	TEA EDA	> 1000	[29]
	$AgNO_3$, Na_2HPO_4	HMT	1000	[30]
	$AgNO_3$, Na_2HPO_4	MEA	42	This study
	$AgNO_3$, H_3PO_4	OLA	20	

evaluated up to a distance cut-off of 12 Å. MEA simulation consisted of 1100 molecules while OLA of 200 due to its large morphology (Fig. 8). Table 3 exhibits the total energy interaction between the Ag^+ cation and MEA/Oleylamine, separately. It is found that the interaction energy of the Ag^+ cation with Oleylamine (E_T = -36.222 Kcal/mol) is greater than that with MEA (E_T = -86.33 Kcal/mol). Therefore, the Oleylamine molecule is strongly attached to the surface of Ag^+, which is directly related to the chain length of the OLA alkyl.

Finally, it is important to compare the sizes of the prepared particles with those reported in the literature. The sizes of Ag_3PO_4 particles prepared in the presence of MEA and OLA as chelating agents used in this study are significantly finely divided about 20 nm for the OLA and 42 nm for the MEA, compared to those prepared elsewhere by varying the chalking agent (Table 4). It is obvious that the affinity of OLA and MEA is more efficient for complexing the Ag^+ ions and consequently retarding their reactivity with the PO_4^{3-} anions, which blocks better the crystal growth of the grains.

CONCLUSIONS

In this study, Ag_3PO_4 nanoparticles have been successfully synthesized via a simple sol gel method using monoethanolamine and oleylamine as chelating agents to control the particles size. The size distribution of the Ag_3PO_4 particles becomes narrower with increasing the surfactant

content (MEA or OLA) with Ag^+. Using XRD, FT-IR, and TEM characterization tools, we showed that OLA provides nanoparticles with 20 nm in size, while MEA gives rise to nanoparticles with a size of 42 nm, but both associated with low concentration of Ag precursor. This result indicates that the ratio between the surfactant and Ag^+ is of great importance the synthesis of nanoscale Ag_3PO_4 particles.

ACKNOWLEDGEMENTS

The Authors would like to acknowledge the support through the R&D Initiative – Call for projects APPHOS phosphates– sponsored by OCP (OCP Foundation, R&D OCP, Mohammed VI Polytechnic University, National Center of Scientific and technical Research CNRST, Ministry of Higher Education, Scientific Research and Professional Training of Morocco MESRSFC) under the project entitled *Development of a phosphate-based photocatalytic reactor prototype for the treatment and recycling of wastewater*, project ID * TRT-NAJ-01/2017*". We thank our sponsors who provided insight, expertise and follow-up that greatly assisted this research.

CONFLICT OF INTEREST

The authors declare that there is no conflict of interests regarding the publication of this paper.

REFERENCES

1. Ibrahim U, Halim A. Heterogeneous photocatalytic degradation of organic contaminants over titanium dioxide : A review of fundamentals, progress and problems. Journal of Photochemistry and Photobiology C : Photochemistry Reviews, 2008; 9:1–12.
2. Guillard C, Disdier J, Herrmann JM, Lehaut C, Chopin T, Malato S, Blanco J. Comparison of various titania samples of industrial origin in the solar photocatalytic detoxification of water containing 4-chlorophenol. J Catalysis Today, 1999; 54:217–228.
3. Sin J, Lam S, Satoshi I, Lee K, Rahman A. Sunlight photocatalytic activity enhancement and mechanism of novel europium-doped ZnO hierarchical micro / nanospheres for degradation of phenol. J Applied Catal. B: Environ, 2014: 148–149:258–268.
4. Taylor P, Lam S, Sin J, Abdullah AZ, Mohamed AR. Degradation of wastewaters containing organic dyes photocatalysed by zinc oxide : a review. Desalination and Water Treatment, 2012; 37–41.
5. Barka N, Qourzal S, Assabbane A, Nounah A, Ait-ichou Y. Factors influencing the photocatalytic degradation of Rhodamine B by TiO_2-coated non-woven paper. J Photochemistry and Photobiology A: Chemistry, 2008; 195:346–351.
6. Chen X, Mao SS. Titanium dioxide nanomaterials : synthesis, properties, modifications, and applications. J Chem Rev, 2007; 107:2891-2959.
7. Bi Y, Ouyang S, Umezawa N, Cao J, Ye J. Facet effect of single-crystalline Ag_3PO_4 sub-microcrystals on photocatalytic properties. J American Chemical Society, 2011; 4:6490–6492.
8. Yi Z, Ye J, Kikugawa N, Kako T, Ouyang S, Stuart-Williams H, Yang H, Cao J, Luo W, Li Z, Liu Y, Withers RL. An orthophosphate semiconductor with photooxidation properties under visible-light irradiation. J Nat Mater, 2010; 9:559–564.
9. Ren J, Chai Y, Liu Q, Zhang L, Dai W. L. Intercorrelated Ag_3PO_4 nanoparticles decorated with graphic carbon nitride: Enhanced stability and photocatalytic activities for water treatment. J Appl Surf Sci, 2017; 403:177-186.
10. Yan X, Gao Q, Qin J, Yang X, Li Y, Tang H. Morphology-controlled synthesis of Ag_3PO_4 microcubes with enhanced visible-light-driven photocatalytic activity. J Ceram Int, 2013; 39:9715–9720.
11. Huang L, Yin S, Guo C, Huang Y, Wang M, Dong Q, Li H, Kimura T, Tanaka M, Sato T. Oleate-assisted room temperature synthesis and high photocatalytic activity of Ag_3PO_4 nanoparticles for no decomposition. J Functional Materials Letters, 2012; 5:2–5.
12. Lin L, Huang M, Long L, Sun Z, Chen D. Facile synthesis, characterization and visible-light photocatalytic performance of Ag_3PO_4. Asian Journal of Chemistry, 2014; 26:7055–7060.
13. Zhang S, Gu X, Zhao Y, Qiang Y. Effect of annealing temperature and time on structure, morphology and visible-light photocatalytic activities Ag_3PO_4 microparticles. J Mater Sci Eng B , 2015; 201:57–65.
14. Dinh C, Nguyen T, Kleitz F, Do T. Large-scale synthesis of uniform silver orthophosphate colloidal nanocrystals exhibiting high visible light photocatalytic activity. J Chem Commun,2011; 47:7797-7799.
15. Vu TA, Dao CD, Hoang TTT, Nguyen KT, Le GH, Dang PT, Tran HTK, Nguyen TV. Highly photocatalytic activity of novel nano-sized Ag_3PO_4 for Rhodamine B degradation under visible light irradiation. Mater Lett, 2013; 92:57–60.
16. Liu Y, Zhu G, Yang J, Yuan A, Shen X. Peroxidase-like catalytic activity of Ag_3PO_4 nanocrystals prepared by a colloidal route. PLoS One, 2014; 9:3–9.
17. Yahia I S, Jilani A, Abdel-wahab MSh, Zahran HY, Ansari MSh, Al-Ghamdi AA,Hamdy MS. The photocatalytic activity of graphene oxide/ Ag_3PO_4 nano-composite: Loading effect. J Optik (Stuttg), 2016; 127:10746–10757.
18. Li X, Zheng R, Luo Q, Wang D, An J, Yin R, Liu Y, Wu D, Han X. Cyclized polyacrynitrile modified Ag_3PO_4 photocatalysts with enhanced photocatalytic activity under visible-light irradiation. J Appl Surf Sc, 2015 ; 356:941–950.
19. Wang P, Li Y, Liu Z, Chen J, Wu Y, Guo M, Na P. In-situ deposition of Ag_3PO_4 on TiO_2 nanosheets dominated by (001) facets for enhanced photocatalytic activities and recyclability. J Ceram Int, 2017; 43:11588–11595.
20. Zhang S, Zhang S, Song L. Super-high activity of Bi^{3+} doped Ag_3PO_4 and enhanced photocatalytic mechanism. J Appl Catal B Environ, 2014; 152–153:129–139.
21. Hou X, Zhang X, Yang W, Liu Y, Zhai X. Synthesis of SERS active Ag_2S nanocrystals using oleylamine as solvent, reducing agent and stabilizer. J Mater Res Bull, 2012; 47:2579–2583.

22. Zhai X, Zhang X, Chen S, Yang W, Gong Z. Oleylamine as solvent and stabilizer to synthesize shape-controlled ZnS nanocrystals with good optical properties. J Colloids Surfaces A Physicochem Eng Asp, 2012; 409:126–129.
23. Dutta M, Mridha S, Basak D. Effect of sol concentration on the properties of ZnO thin films prepared by sol – gel technique. J Applied Surface Science, 2008; 254:2743–2747.
24. Yang W, Wang C, Arrighi V. Effects of amine types on the properties of silver oxalate ink and the associated film morphology. J Mater Sci Mater Electron, 2018; 29:20895–20906.
25. Xu W, Wang T. Synergetic effect of blended alkylamines for copper complex ink to form conductive copper films. Langmuir, 2017; 33:82-90.
26. Sansotta S, Zahn D, Sansotta S, Zahn D. Solvation structure and dynamics of Ag in aqueous ammonia solutions : A molecular simulation study solvation structure and dynamics of Ag^+ in aqueous ammonia solutions : a molecular simulation study. Journal of Chemical Physics, 2017; 114506.
27. Amornpitoksuk P, Intarasuwan K, Suwanboon S, Baltrusaitis J. Effect of phosphate salts (Na_3PO_4, Na_2HPO_4, and NaH_2PO_4) on Ag_3PO_4 morphology for photocatalytic dye degradation under visible light and toxicity of the degraded dye products Ind. Eng. Chem. Res., 2013; 52:17369-17375.
28. Yang Z.M, Liu Y.Y, Xu L, Huang G.F, Huang W.Q. Facile shape-controllable synthesis of Ag_3PO_4 photocatalysts. Mater. Lett., 2014; 133:139-142.
29. Xu Y.S, Zhang W.D. Morphology-controlled synthesis of Ag_3PO_4 microcrystals for high performance photocatalysis. CrystEngComm., 2013; 15:5407-5411.
30. Wang K, Xu J, Hua X, Li N, Chen M, Teng F, Zhu Y, Yao W. Highly efficient photodegradation of RhB–MO mixture dye wastewater by Ag_3PO_4 dodecahedrons under acidic condition. J. Mol. Catal. A: Chem., 2014; 393:302-308.